



ORIGINAL ARTICLE

Synthesis, hemorheological and antifibrotic activity of newly synthesized 3-acetyl-2,4,6-trimethylpyridine derivatives



Zarina Shulgau^{a,*}, Alena Stalinskaya^c, Shynggys Sergazy^{a,b},
Aigerim Zhulikeyeva^a, Yevgeniy Kamyshanskiy^{a,e}, Alexander Gulyayev^{a,b},
Yerlan Ramankulov^a, Ivan Kulakov^{a,d}

^a National Center for Biotechnology, 13/5 Kurgalzhynskoe Road, 010000 Astana, Kazakhstan

^b National Laboratory Astana, Nazarbayev University, Astana, Kazakhstan

^c Institute of Environmental and Agricultural Biology (X-Bio), University of Tyumen, 23 Lenina St., Tyumen 625003, Russia

^d Center for Nature-Inspired Engineering, Tyumen State University, 15a Perekopskaya St., 625003 Tyumen, Russia

^e Clinic of Medical University "MUK" NCJSC, Karaganda, Kazakhstan

Received 27 January 2023; accepted 15 March 2023

Available online 22 March 2023

KEYWORDS

Pyridine (and collidine) derivatives;
3-acetyl-2,4,6-trimethylpyridine;
Pulmonary fibrosis;
Bleomycin;
Blood rheology;
Hyperviscosity

Abstract Pyridine derivatives still attract the attention of many researchers for their comprehensive biological research, possible promotion to the pharmaceutical market in order to be used as effective drugs. In this article, based on the well-known and fairly accessible in terms of laboratory synthesis of the 3-acetyl derivative of collidine, we carried out several simple chemical modifications to obtain new collidine derivatives not previously described. The structure of the synthesized compounds was confirmed by ¹H- and ¹³C NMR spectroscopy. A biological screening of the synthesized compounds for hemorheological activity was carried out on an in vitro blood hyperviscosity model. It was shown that pronounced hemorheological activity was established for compounds **3**, **4** and **5**. Compound **4** also showed a pronounced antifibrotic effect in an experimental model of pulmonary fibrosis induced by intratracheal administration of bleomycin to rats. In an experimental model of pulmonary fibrosis in rats, the formation of a hyperviscosity syndrome was also observed, and blood viscosity decreased when compound **4** was administered to animals.

© 2023 The Author(s). Published by Elsevier B.V. on behalf of King Saud University. This is an open access article under the CC BY-NC-ND license (<http://creativecommons.org/licenses/by-nc-nd/4.0/>).

* Corresponding author.

E-mail addresses: shulgau@biocenter.kz (Z. Shulgau), kamyshanskiy84@mail.ru (Y. Kamyshanskiy), i.v.kulakov@utmn.ru (I. Kulakov).
Peer review under responsibility of King Saud University.



1. Introduction

It is known that many nitrogen-containing heterocyclic compounds are used in pharmaceutical practice as broad-spectrum drugs (Soldatenkov, A.T.; Kolyadina, N.M.; Shendrik, I.V. *Fundamentals of Organic Chemistry of Medicinal Substances; Chemistry: Moscow, Russia, 2001*; Asif, 2017; Kerru et al., 1909). Among nitrogen-containing heterocycles, pyridine derivatives constitute a unique group that includes about 5% of all known drugs. Pyridine-based compounds demonstrate higher bioactivity, lower toxicity, advanced systemic and/or excellent selectivity in comparison to their benzenoid counterparts due to smaller hydrophobic constant (0.65 for pyridine vs 1.96 for benzene). Pyridine derivatives are the part of the vital vitamins B₃ (PP) and B₆ (Fig. 1), that play an important role in human metabolism and widely used in medical practice as drugs with a variety of therapeutic effects (antibacterial, antituberculosis, antidepressant, antihistamine, analgesic, psychotropic, nootropic and others) (Available online, 2022; Mashkovsky, 2017; Alousi et al., 1979; Fox, 1952; Ward et al., 1983). Pyridine derivatives are also used in agriculture as effective fungicides, herbicides and growth-stimulating substances (Melnikov, 1987; Shimanskaya and Leitis, 1989; McDougall, 2014). Pronounced pharmacological effect of active substances is due to continuous maintenance of pharmacophores in an active state, since a change in their position or the formation of additional bonds can change the spectrum of activity exhibited by the substance. The presence of hydroxyl (or amino-) and alkyl groups with different electron-donor properties in pyridine derivatives leads to antioxidant activity (Kulakov et al., 2015; Kulakov et al., 2014; Kulakov et al., 2018; Palamarchuk et al., 2021). For example, emoxypine (2-ethyl-6-methyl-3-hydroxypyridine succinate **1**, Fig. 1) has antioxidant and membrane-protective properties (Available online, 2022). Its chemical structure resembles that of pyridoxine (a type of vitamin B₆). Recently, a close analogue of emoxypine – 2,4,6-trimethyl-3-hydroxypyridine nitrosuccinate **2** (Fig. 1) demonstrating better effectiveness was synthesized and patented (Fedorov et al., (n.d.)). This derivative of collidin is a promising anti-ischemic agent with a vasodilatory effect, which can exhibit a protective effect in barotraumatic injuries and gunshot wounds by inhibiting the processes of occurrence and development of secondary necrosis (Gilmanov et al., 2012).

The introduction of new pharmacophore groups into the structure of a bioactive molecule and the study of the effect of chemical modifications on the biological activity of compounds is one of the primary tasks of organic synthesis. To this day, the search and optimization of the conditions for many reactions is being carried out in order to increase yields and simplify synthesis protocols. Properly selected inexpensive and readily available reagents greatly alleviate this task. Pyridine carbonyl derivatives are a convenient basis for constructing structural derivatives with desired pharmacological properties.

Our previous studies on the modification of pyridine acetyl derivatives also have revealed structures with antituberculous, antibacterial, antiviral, and analgesic activity (Stalinskaya et al., 2022; Oleshchuk et al., 2019; Kulakov et al., 2017; Oleshchuk et al., 2020). The purpose of this work is to carry out some chemical modifications of 3-acetyl-2,4,6-trimethylpyridine **3**. Back in 1947, Dornow A. published a work (Dornow and Machens, 1947), which provides a very simple one-stage method for the synthesis of 3-acetyl-2,4,6-trimethylpyridine **3**. Besides,

there are two more modern methods in the literature for obtaining 3-acetyl-2,4,6-trimethylpyridine **3** under palladium-catalysed conditions (Lejon et al., 2005) and under transition-metal catalyst-free conditions (Song et al., 2016). However, after the publication of the synthesis of this 3-acetyl derivative of collidin, there is practically no information on its possible chemical modification in the literature. There is only information about modifications of collidin (Abblard et al., 1972; Van Rijn, 1926) and few reactions of 3-acetyl-2,4,6-trimethylpyridine **3** to provide α -branched ketones (Frost et al., 2015; Akhtar et al., 2017). The probability of the antioxidant effect of pyridine derivatives is estimated as relatively high and has been proven for a number of new compounds (Kaddouri et al., 2020), and the types of biological activity pathophysiologically related to the antioxidant effect can be considered as targets for testing new compounds.

The presence of antiradical activity in compounds suggests a fairly wide spectrum of their biological activity. The active participation of rheological mechanisms in circulatory disorders has been proven (Cecchi et al., 2009). Rheological occlusion is considered as an initiating factor of plasma coagulation mechanisms leading to thrombus formation. The deterioration of the viscoelastic properties of erythrocytes leads to a deterioration in microcirculation, which leads to a decrease in local blood flow and tissue hypoxia. It is known that hemodynamic disturbances are determined not only by the state of platelet-vascular hemostasis, but also by the rheological properties of blood (Roitman, 2003), therefore, it is of interest to study the possibilities of the pharmacological effect of synthesized compounds on the viscosity properties of blood.

Previously it has been shown that excessive lipid peroxidation increases viscosity of blood (Nemeth et al., 2021; Caprari et al., 2019). Successful attempts to prevent the negative effect of lipid peroxidation on the rheological properties of erythrocytes has been made with usage of antioxidants (Becatti et al., 2016; Jian et al., 1993). This prompted us to screen the synthesized compounds with assumed antioxidant properties for rheological activity.

Thus, screening for biological activity of new modifications of 3-acetyl-2,4,6-trimethylpyridine **3**, carried out *in vitro* on a model of hemorheology disorders and *in vivo* on a model of pulmonary fibrosis in this work logically complements the main goal.

2. Results

2.1. Chemistry

One way to modify the free acetyl group in the third position of pyridine **3** is to reduce it to an alcohol group (De Martino et al., 2005; Stepanenko et al., 2007; Truppo et al., 2007; Itsuno, 1998). We carried out the reduction of the acetyl group of 3-acetyl-2,4,6-trimethylpyridine **3** in the presence of a 2-fold excess of sodium borohydride in an aqueous solution of ethanol (Scheme 1).

According to the data of gas chromatography-mass spectrometry, the reaction proceeds under the given conditions with complete conversion of the starting pyridine, while the actual yield of the reduced product is 90%. The resulting pyr-

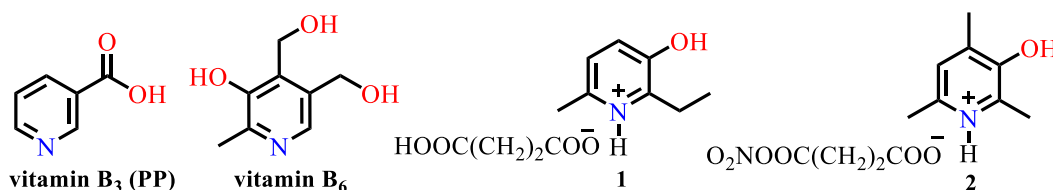
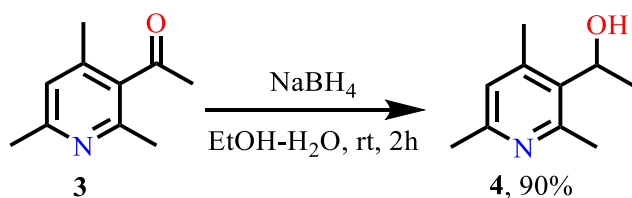


Fig. 1 Structural formulas of drugs of the pyridine series.



Scheme 1 Reduction of acetyl group.

idine hydroxy derivative **4** was isolated as a mixture of enantiomers, it is a white crystalline powder, easily soluble in most organic solvents. It also has good solubility in water (10 mg in 0.5 ml of H₂O (pH = 7, at 20 °C), which can positively affect its bioavailability. It should be noted that the structure of compound **4** is given in the article (Lauber and Stahl, 2013), where it is used as the starting product for the reverse reaction of the oxidation of alcohol **4** to ketone **3**. However, any information about the method of its preparation, physicochemical constants and spectral characteristics in cited work (Huang et al., 2010) are completely absent.

For carbonyl groups, the reaction with N-nucleophiles of various structures is characteristic and specific. An example of this can be oximes that have useful practical properties, including a wide range of biological activity, including antitubercular, cytotoxic, antiviral, anti-inflammatory, and other properties. (a Costa et al., 2020; Abele et al., 2003; Latif et al., 2019; Schepetkin et al., 2021). In addition, pyridine oximes are used as antidotes for poisoning with organophosphorus compounds (Jokanovic and Prostran, 2009). In this regard, we carried out the reaction of nucleophilic substitution of the carbonyl group of 3-acetyl-2,4,6-trimethylpyridine **3** with an oxime group by reacting it with hydroxylamine (Scheme 2).

According to the data of chromato-mass spectrometry, the reaction under the given conditions proceeds with the formation of oxime **5** in the form of a mixture of *E*- and *Z*-isomers with an approximate ratio of 3:2 and close retention times ($t_R = 7.53$ and 7.80 min), which did not allow them to be divided into separate individual isomers. The ratio and correlation of the mixture of *E*- and *Z*-isomers was carried out using ¹H NMR spectroscopy. When analyzing the ¹H NMR spectrum of a mixture of isomers, it was found that when integrating the singlets of all 4 methyl groups, as well as the singlets of the H-5 proton and the hydroxyl proton of oxime **5**, all signals are duplicated while maintaining the overall ratio of 3:2. The assignment of isomers was made on the assumption that the

proton of the hydroxamic fragment of the *Z*-isomer, due to spatial factors of a rigid geometric structure, enters the field of action of the anisotropy cone of the aromatic pyridine ring, which leads to its shift to a stronger field in the region of 10.55 ppm. compared to the same hydroxyl proton of the *E*-isomer (11.07 ppm). Based on this, it was concluded that the minor isomer belongs to the *Z*-form. A similar splitting and duplication of signals with different intensities is also observed in the ¹³C NMR spectrum. The reaction yield is 76%.

Another promising trend in the chemistry of pyridine derivatives is the preparation of pyridine N-oxides. Pyridine N-oxides have an extremely interesting reactivity (Katritzky and Lagowski, 1967; Oae and Ogino, 1977; Habib et al., 2023), which differs significantly from the reactivity of both pyridines themselves and quaternary pyridinium salts. The N-oxide group, depending on the conditions, facilitates the reactions of both electrophilic substitution and nucleophilic substitution at the α - and γ -positions.

Given the above, it was of interest to us to obtain a synthon with an increased reactivity for its further chemical transformations. The synthesis of the required 3-acetyl-2,4,6-trimethylpyridine N-oxide **6** was carried out by treating 3-acetyl-2,4,6-trimethylpyridine **3** with a solution of hydrogen peroxide in acetic acid (Scheme 3).

The progress of the reaction was monitored by chromatographic analysis. So, after 5 h of boiling, trace amounts of unreacted 3-acetyl-2,4,6-trimethylpyridine **3** and the main amount of the corresponding N-oxide **6** remained in the reaction mixture. The actual reaction yield was 70%.

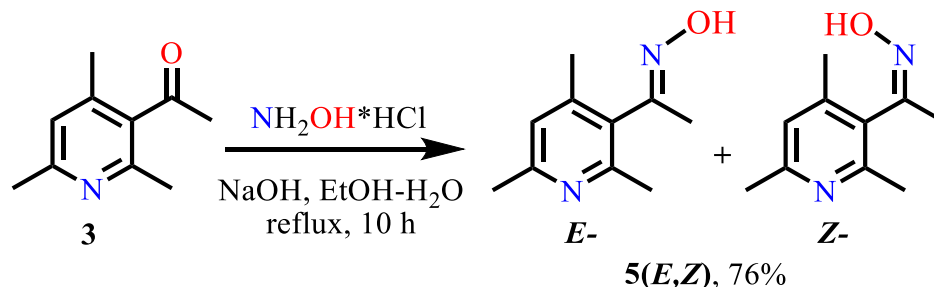
For ease of use and improvement of the water solubility of 3-acetyl-2,4,6-trimethylpyridine **3**, it was decided to convert it to the corresponding hydrochloride **7** (Scheme 4).

Thus, based on laboratory-available 3-acetyl-2,4,6-trimethylpyridine **3**, we carried out several simple chemical modifications in order to determine a further possible direction of synthesis to obtain new structural derivatives of collidine and to establish the “structure–activity” relationship.

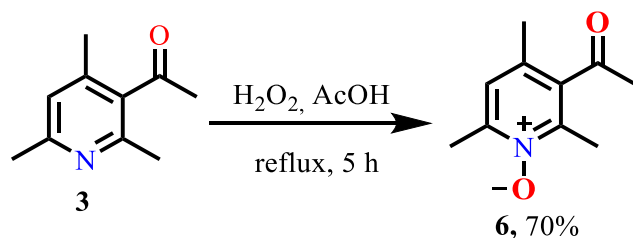
2.2. Biological activity

2.2.1. Hemorheological activity in an *in vitro* blood hyperviscosity model

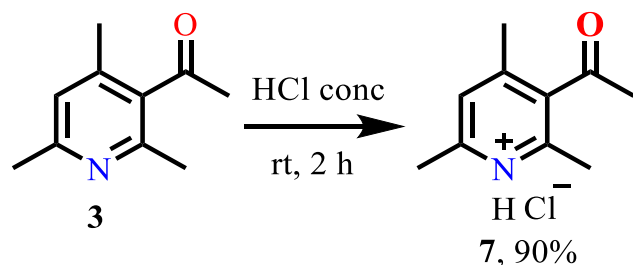
In experiments on the study of hemorheological activity of samples (Table 1), it was found that incubation of blood for 60 min at a temperature of 43.0 °C led to a significant increase in blood viscosity at various spindle speeds from 2 to 60 rpm, which indicates the formation of blood hyperviscosity.



Scheme 2 Nucleophilic substitution of the carbonyl group of 3-acetyl-2,4,6-trimethylpyridine **3** with an oxime group.



Scheme 3 Synthesis of synthon **6** by treating **3** with a solution of hydrogen peroxide in acetic acid.



Scheme 4 Conversion of 3-acetyl-2,4,6-trimethylpyridine **3** to hydrochloride **7**.

Table 1 Histomorphometric characteristics of the degree of fibrosis.

Indicator	Intact animals (n = 4)	Control (n = 4)	Compound 4 (n = 4)
< 1% (0, none) (n,%)	4/100	–	–
< 10% (I mild degree) (n,%)	–	–	1/25
< 30% (II moderate degree) (n,%)	–	1/25	2/50
> 30% (III severe degree) (n,%)	–	3/75	1/25
M ± SD	2.6 ± 0.3	59.4 ± 11.8	18.8 ± 4.4

Fig. 2 shows that compounds **3**, **4** and **5** have hemorheological activity under the conditions of the in vitro model of blood hyperviscosity. Compound **4** was able to significantly reduce blood viscosity compared to low and medium shear controls (2 to 20 revolutions per minute $p < 0.05$). Compound **3** was able to significantly reduce blood viscosity compared to low, medium and high shear controls (from 2 to 60 revolutions per minute $p < 0.05$, except for speed 6, where the significance level was $p = 0.1184$). Compound **5** was able to significantly reduce blood viscosity compared to low and medium shear controls (2 to 20 revolutions per minute $p < 0.05$). These compounds were not able to restore normal viscosity, however.

Compound **4**, among the other studied compounds, looked as the most promising, both in terms of its state of aggregation (white crystalline powder), ease of synthesis and preparative

purification, and in terms of the strength of the hemorheological effect. Compound **5** was tested as a mixture of geometric isomers (E- and Z-forms) due to the rather complicated procedure for their separation. This fact may create further certain difficulties at the stage of further in-depth bio-screening due to their different pharmacological properties.

Therefore, compound **4** was chosen for more in-depth studies *in vivo*.

Fig. 2 shows that compounds **6** and **7** do not have any hemorheological activity under the conditions of the in vitro model of blood hyperviscosity.

Thus, analysis of the bioscreening of the synthesized compounds 3–7 showed that only the modification of the carbonyl group in 3-acetyl-2,4,6-trimethylpyridine **3** to alcohol and oxime groups led to a significantly higher hemorheological activity of the compounds.

2.2.2. Histopathological examination

Compound **4** was chosen for further studies of antifibrotic and hemorheological activity in an experimental model of pulmonary fibrosis in rats induced by intratracheal administration of bleomycin.

Pulmonary fibrosis is a histopathological pattern of damage to the lungs of animals in an experimental study, which is a stress-induced bleomycin violation of the histoarchitectonics of the respiratory sections with excessive deposition of extracellular connective tissue matrix (collagen type I and III) (Gross and Hunninghake, 2001). Type I collagen (mature collagen) is the most abundant collagen, which is a structural component of connective tissue and the predominant component of the interstitial membrane, which forms the structural and mechanical basis (matrix) of bones, skin, tendons, cornea, blood vessel walls, and other connective tissues (Amirrah et al., 2022). Type III collagen (other names: immature collagen, reticulin) is the second most common collagen, expressed in early embryos and throughout embryogenesis, in adults it is the main component of the extracellular matrix, distributed in the wall of large blood vessels, reticular fibers of hematopoietic organs (Liu et al., 1997).

In our experimental study, the degree and stage of fibrosis are not identical concepts, but reflect two independent phenotypes of fibrotic damage to lung tissue.

2.2.2.1. Comparative histomorphometric characteristics of the degree of pulmonary fibrosis in the experimental groups of the study. The results of the histomorphometric characteristics of the degree of fibrosis are presented in Table 1. In the intact group, there were no histoarchitectonic disorders associated with fibrosis. The average value of the area of fibrosis in the intact group was $2.6 \pm 0.3\%$.

In the control group, the average value of the area of fibrotic damage to lung tissue was 59.4 ± 11.8 , which is typical for diffuse damage. Severe fibrosis was observed in 3 cases (75%), moderate in 1 case (25%), mild fibrosis and cases with no fibrosis were identified.

In the group that received compound **4**, the average value of the area of fibrous lesions of the lung tissue was $18.8 \pm 4.4\%$. In the group administered compound **4**, a mild degree of fibrotic damage to the lungs was detected in 25% of cases, moderate in 50%, and a severe degree was noted only in 1 case, which amounted to 25%.

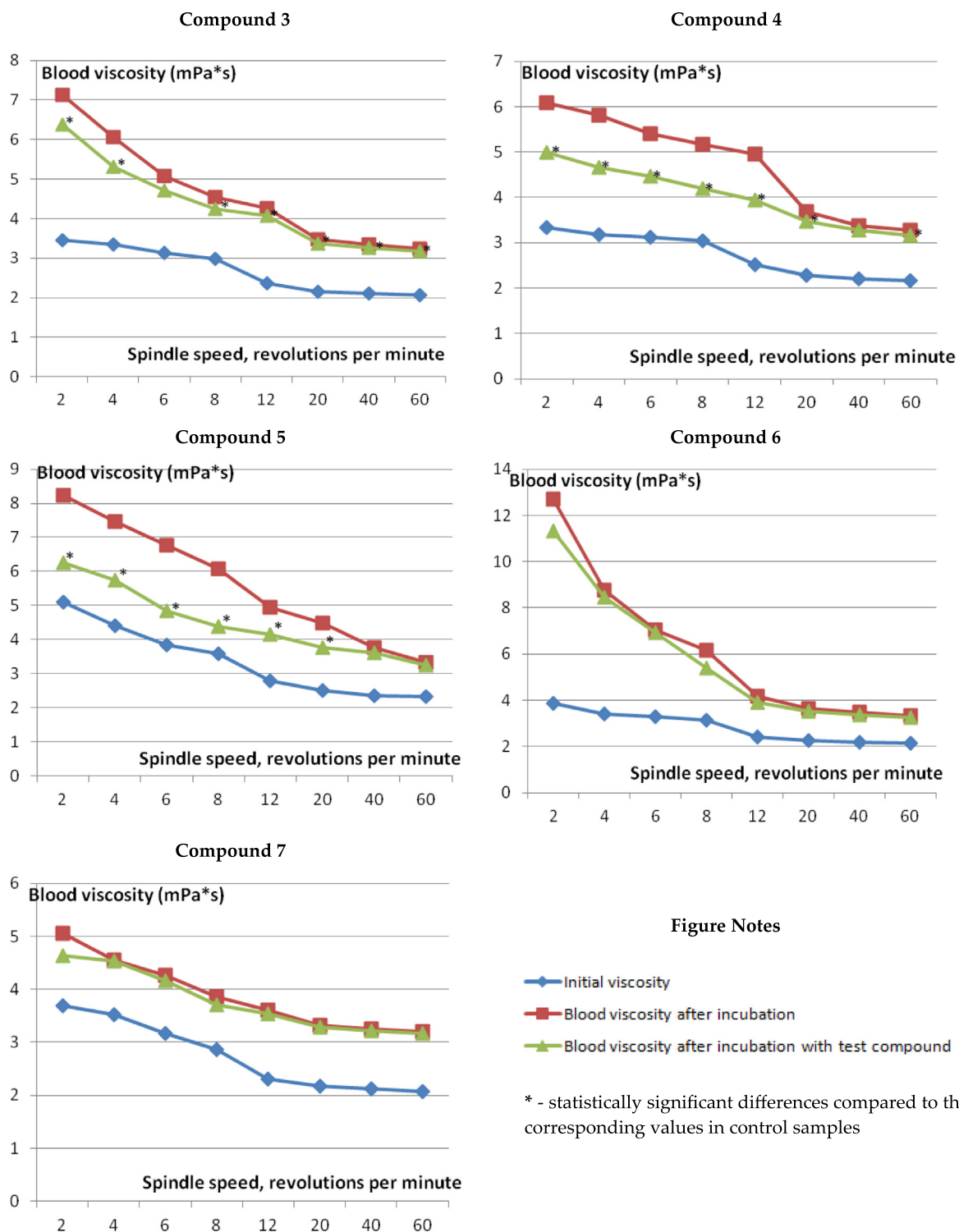


Fig. 2 Effect of studied samples on blood viscosity (mPa*s) at different spindle speeds in an in vitro blood hyperviscosity model.

2.2.2.2. Comparative histomorphometric characteristics of the stage of pulmonary fibrosis (histopattern of fibrous tissue) in the experimental groups of the study. The results of the histomorphometric characteristics of the stage of fibrosis are presented in Table 2.

In the intact group, the formation of fibrosis foci (stage FLO) was not detected. In all cases, only single peripheral short linear fibers of type I collagen were observed in the subepithelial zone of the central bronchi and peripheral bronchioles, as well as in the wall of large vessels. Type III collagen was

Table 2 Histomorphometric characteristics of the stage of fibrosis.

Indicator	Intact animals (n = 4)	Control (n = 4)	Compound 4 (n = 4)
FL0 (n/%)	4/100	–	–
FL1 (n/%)	–	–	1/25
FL2 (n/%)	–	1/25	1/25
FL3 (n/%)	–	2/50	2/50
FL4 (n/%)	–	1/25	–
M ± SD	–	40.4 ± 11/	69.4 ± 16/
(collagen type III/collagen type I)	–	50.4 ± 15	31.6 ± 9

represented by thin filamentous structures distributed in the alveoli and respiratory bronchioles.

In the control group, the histological pattern of fibrous tissue was characterized by the relative predominance of mature type I collagen in the foci of lung tissue fibrosis in 75% of cases. In 2 cases (50%) the fibrosis pattern corresponded to the FL3 stage, in one case (25%) FL4. The focal nature of the distribution of mature type I collagen among the diffuse pattern of immature resorbable collagen fibers (stage FL2) was detected only in 1 case (25%). There were no cases with the stage of fibrosis with a minimum amount of FL1 and the absence of FL0 of mature stable type I collagen in the control group.

In the group with compound 4, the pattern of fibrous tissue corresponded to FL1 in 25% of cases. The stage of fibrous tissue with a moderate predominance of reticulin FL2 was observed in 25% of cases. Stage FL3 with a moderate predominance of mature collagen fibers was detected in group 4 in 50% of cases. Cases with a pronounced predominance (stage FL4) of mature collagen were not detected, in contrast to the control group.

2.2.2.3. Comparative histomorphometric characteristics of the inflammatory pattern and interstitial edema. The results of the histomorphometric characteristics of the inflammatory pattern and interstitial edema are presented in Table 3.

In the intact group, in all cases, the morphological pattern was represented by thin interalveolar septa without signs of

interstitial edema or inflammatory infiltration by immune cells. In the intact group (sham-operated animals), in all cases, the morphological pattern was represented by thin interalveolar septa without signs of interstitial edema or inflammatory infiltration by immune cells.

In the control group, chronic active inflammation was detected in 100% of cases, of which: 1) infiltration with polymorphonuclear leukocytes: diffuse in 100% of cases (mean value 323.8 cells); (2) plasma cell infiltration, macrofocal and diffuse (75% and 25% of cases, respectively), mean 219.8 cells. There were no cases with mild infiltration by immunoinflammatory cells. The average number of multinucleated giant cells was 27.3 cells. There were single macrophages with cytoplasmic inclusions (mean number 3.8 cells). In the control group, in all cases (100%), there was an acute interstitial injury with diffuse perivascular edema involving 84.5% of the vessels (Fig. 3).

In the group with compound 4, no active chronic inflammatory process was detected in all cases. Moderate chronic non-specific inflammation with moderate plasmacytic infiltration was observed in 100% of cases (average granulocyte count 28.5 plasma cells – 150.3). Giant multinucleated cells averaged 0.8 cells, were single or absent (75% and 25% of cases, respectively). Macrophages with cytoplasmic inclusions (foam cells) were observed in large numbers (mean number 28.8) in 100% of cases. There was a histomorphometric picture of moderate edema (21.8% of vessels).

2.2.3. Results of the study of hemorheological activity of compound 4 in experimental pulmonary fibrosis in rats

To date, there is evidence that bleomycin, in the process of modeling pulmonary fibrosis, in addition to damaging alveolar epithelial cells, can change hemorheological parameters. Thus, it is known that bleomycin can interact with the vascular endothelium, which leads to endothelial-mediated inflammation and increased adhesion of neutrophils (Williamson et al., 2016). Dygai AM et al (Dygai et al., 2011) found that the development of diffuse pulmonary fibrosis with intratracheal administration of bleomycin was accompanied by hyperplasia of bone marrow hematopoiesis and leukocytosis in peripheral blood. Later (Rathinasabapathy et al., 2018), it was found that, in parallel with the initiation of pulmonary fibrosis in the peripheral circulation, bleomycin slightly increases the number of leukocytes and significantly increases the number of platelets. These facts are the basis for the

Table 3 Histomorphometric characteristics of the inflammatory pattern and interstitial edema.

Indicator	Intact animals (n = 4)	Control (n = 4)	Compound 4 (n = 4)
Edema*	0	84,5 ± 5,8	21,8 ± 6,4
Polymorphonuclear leukocytes**	0	323,8 ± 12,6	28,5 ± 14,5
Plasma cells**	0	219,8 ± 143,4	150,3 ± 48,0
Multinucleated giant cells***	0	27,3 ± 6,6	0,8 ± 0,5
Macrophages with cytoplasmic inclusions (foam cells)***	0	3,8 ± 1,7	28,8 ± 9,3

* % of vessels with edema in the perivascular space.

** per 1000 of all cells in the entire area of the histological section.

*** average number of cells per 10 fields of view x200.

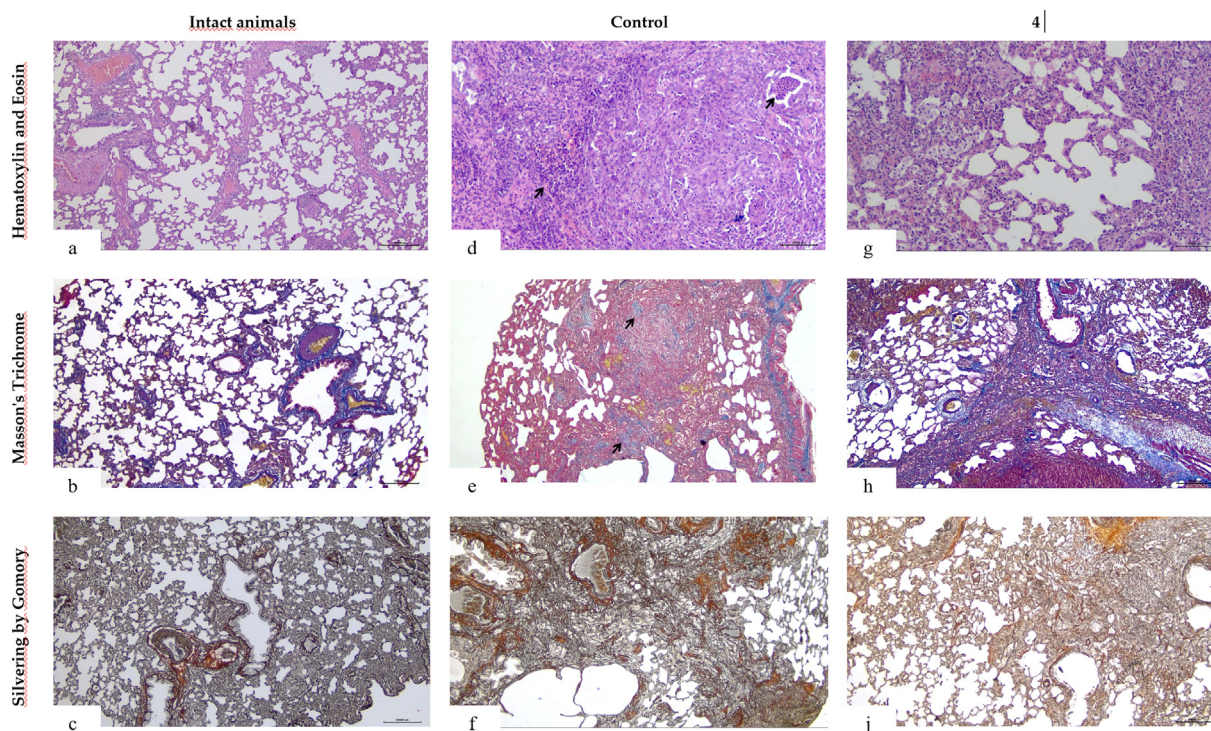


Fig. 3 Microphotographs of the lungs of rats a - Intact animals. The morphological pattern is represented by thin interalveolar septa without signs of edema or inflammatory infiltration (hematoxylin and eosin stain, $\times 40$); b - Intact animals. Morphological pattern of single peripheral fibers of mature non-resorbable collagen I in the respiratory compartment and the wall of large vessels (Masson's trichrome stain, $\times 40$); c - Intact animals. Histological pattern characterized by uniform formation of immature resorbable collagen III fibers (Gomory silver stain, $\times 40$); d - Control (untreated). Inflammatory pattern with diffuse infiltration (score 3, severe inflammation) of polymorphonuclear leukocytes (black arrow) and plasma cells (hematoxylin and eosin stain, $\times 40$); e - Control. Morphological pattern of pulmonary fibrosis ($> 30\%$ of the area, stage III, severe) with the formation of mature non-resorbable type I collagen (black arrows) and diffuse impairment of lung histoarchitecture (Masson's trichrome stain, $\times 40$); f - Control. Morphological pattern of diffuse formation of immature resorbable type III collagen fibers (immature collagen, reticulon) (Gomory silver stain, $\times 40$); g - **4**. Morphological pattern of mild chronic nonspecific inflammation with accumulation of macrophages (hematoxylin and eosin stain, $\times 40$); h - **4**. Histological pattern characterized by focal formation of mature non-resorbable type I collagen fibers (Masson's trichrome stain, $\times 40$); j - **4**. Morphological pattern of diffuse formation of immature resorbable type III collagen fibers (silver staining according to Gomory, $\times 40$).

Table 4 Effect of **4** on blood viscosity (mPa*s) at different spindle speeds in animals with experimental pulmonary fibrosis induced by intratracheal administration of bleomycin.

Study group	Blood viscosity (mPa*s) at various spindle speeds, revolutions per minute							
	2	4	6	8	12	20	40	60
Intact animals, n = 4	6.40 \pm 0.11	4.61 \pm 0.15	3.90 \pm 0.11	3.52 \pm 0.08	3.04 \pm 0.08	2.62 \pm 0.06	2.29 \pm 0.10	2.25 \pm 0.10
Control, n = 4	7.70 \pm 0.46	6.13 \pm 0.33	5.41 \pm 0.16	4.59 \pm 0.04	3.84 \pm 0.23	3.05 \pm 0.17	2.44 \pm 0.06	2.26 \pm 0.06
4 , n = 4	p1 = 0.0499	p1 = 0.0081	p1 = 0.0003	p1 = 0.00001	p1 = 0.0236	p1 = 0.0763	p1 = 0.2959	p1 = 0.9798
	4.78 \pm 0.44	4.07 \pm 0.12	3.72 \pm 0.15	3.45 \pm 0.08	2.97 \pm 0.11	2.48 \pm 0.11	2.33 \pm 0.09	2.30 \pm 0.09
	p1 = 0.0036	p1 = 0.0447	p1 = 0.3536	p1 = 0.5797	p1 = 0.6082	p1 = 0.2618	p1 = 0.8063	p1 = 0.7519
	p2 = 0.0155	p2 = 0.0108	p2 = 0.0019	p2 = 0.0001	p2 = 0.0640	p2 = 0.0926	p2 = 0.4113	p2 = 0.7260

Note:

n is the number of samples in a group; p is the significance level;

p1 < 0.05 - statistically significant differences compared to the corresponding values in intact animals;

p2 < 0.05 - statistically significant differences compared to the corresponding values in control animals.

assumption of a probable change in hemorheological properties when modeling pulmonary fibrosis using bleomycin.

The results of the study of the rheological properties of the blood of animals with experimental pulmonary fibrosis

induced by intratracheal administration of bleomycin are presented in Table 4 and Fig. 4. It can be seen from the presented data that experimental pulmonary fibrosis induced by bleomycin leads to the formation of a syndrome of increased blood

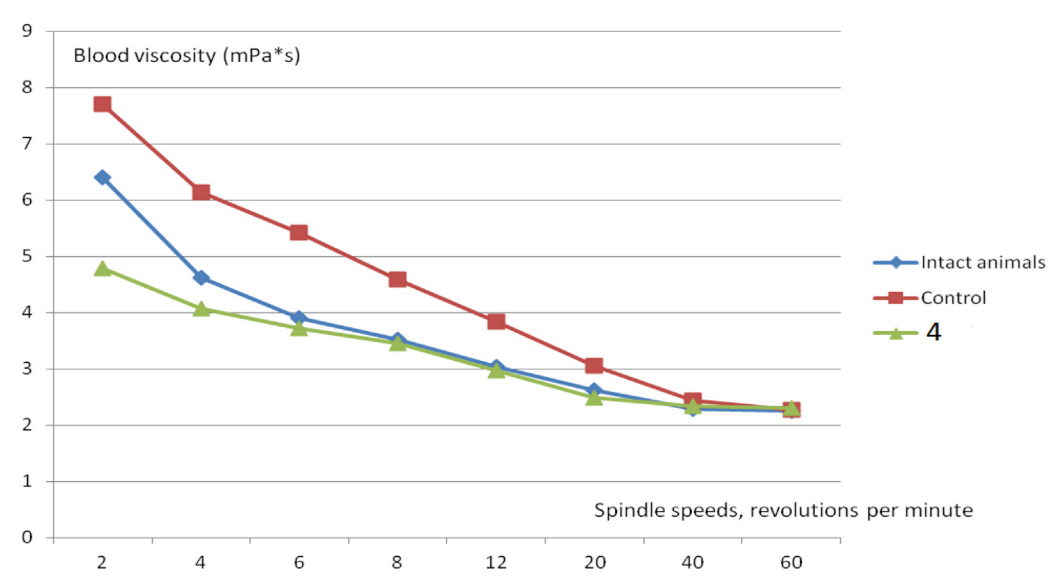


Fig. 4 Effect of **4** on blood viscosity (mPa*s) at different spindle speeds in animals with experimental pulmonary fibrosis induced by intratracheal administration of bleomycin.

Table 5 The level of viability of neonatal human dermal fibroblasts (in % to control) under in vitro conditions under the influence of compound **4** in the MTT test.

Sample concentration, mg/ml cells in nutrient medium	Compound 4
1	94,9
0,5	92,9
0,25	116,6
0,125	105,6
0,0625	100,7
0,03125	110,3
Control	100,0

viscosity. The use of compound **4** reduces the severity of blood hyperviscosity to the parameters characteristic of intact animals.

2.2.4. Studies of cytotoxic properties

For a possible assessment of the toxicity of the test compounds, a cytotoxicity test (MTT-test) was carried out in a culture of human fibroblasts, which allows us to conclude that there is no negative effect of the samples on human fibroblast cells.

The **Table 5** shows the average values of cell survival (in % of control) for three measurements.

The table shows that compound **4** has a moderate dose-dependent cytotoxicity against neonatal human dermal fibroblast cell culture, which manifests itself mainly at high concentrations. At the same time, in the concentration range from 0.03125 to 0.25 mg/ml of cells, compound **4** does not exhibit cytotoxic effects. Since the physiologically achievable concentrations for most pharmacologically active compounds do not exceed 10–5 g/ml (0.01 mg/ml), it can be argued that compound **4** at physiological concentrations does not have cytotoxic properties in relation to the cell culture of neonatal human dermal fibroblasts.

3. Discussion

It has been established that **4** improves the pattern of lung tissue due to antifibrotic and anti-inflammatory effects. In groups using **4**, the degree of pneumofibrosis is significantly less than in the control group ($p < 0.05$), fibrosis is located focally, with a predominance of immature resorbable collagen fibers (collagen type III, reticulin) (**Fig. 2-h,j**), in contrast to the control group, where diffuse formation of fibrotic structures was noted with a predominance of mature non-resorbable type I collagen (**Fig. 2-e,f**). Also in group **4**, the semi-quantitative assessment of granulocytic infiltration and plasma cells was less than in the control group ($p < 0.05$), where large-focal and diffuse inflammatory infiltration was observed, consistent with active chronic inflammation (**Fig. 2-d**).

In group **4**, among the areas of immature fibrous tissue, there were more than in the control group the number of active macrophages with intracytoplasmic inclusions (**Fig. 3,g**) according to the cytological pattern characteristic of foam cells with high autophagy function and a smaller number of multinucleated giant cells ($p < 0.05$). We believe that the use of **4** improves macrophage activity, which improves the local microenvironment of the connective tissue matrix due to the resorption of damaged tissue fragments and antigens with a pro-inflammatory effect. It is possible that the antifibrotic effect of **4** is associated with the formation of a favorable regional microenvironment with high autophagy activity.

It was revealed that the formed fibrous tissue has different structural patterns with qualitative and semi-quantitative differences in the ratio of type I and type III collagen. In the control group, fibrous tissue was predominantly formed by type I collagen, in contrast to group **4**, where immature resorbable type III collagen predominated. Perhaps the use of **4** indirectly reduces the relative amount of fibrous tissue by preventing or inhibiting the transformation of reticulin into mature type I collagen.

In group 4, no histological picture of the locoregional immunosuppressive phenomenon was revealed. In a previously published work, it was shown that the use of immunosuppressive drugs is accompanied by active biosynthesis of immature collagen (reticulin (collagen type III)) with a relatively reduced amount of mature collagen (Paul et al., 2014). However, in our work it was found that in the group using 4 there was a decrease in the total amount of fibrous tissue, consisting of both immature and mature collagen. In group 4, on the one hand, there is a statistically significant decrease in active pro-inflammatory immune cells, on the other hand, an increase in active phagocytic macrophages, in contrast to the control group. We believe that 4 has a locoregional immunomodulatory effect with the formation of a favorable immunological microenvironment with an antifibrotic effect.

It can be seen from the obtained results that blood viscosity in experimental pulmonary fibrosis induced by bleomycin increases, and blood viscosity increases mainly at medium and low spindle speeds (from 2 to 12 revolutions per minute $p < 0.05$ in comparison with intact animals), at high spindle speeds, blood viscosity does not differ from the corresponding parameters in intact animals (from 20 to 60 revolutions per minute $p > 0.05$ in comparison with intact animals). An increase in blood viscosity is formed as a result of unidirectional shifts in rheological parameters: an increase in hematocrit, plasma viscosity, an increase in erythrocyte aggregation and a decrease in their deformability. It is known that blood viscosity at low speeds depends mainly on erythrocyte aggregation, while at high speeds it is determined mainly due to the deformability of erythrocytes (Plotnikov et al., 2011). From the data obtained, it can be assumed that under conditions of experimental pulmonary fibrosis induced by bleomycin, blood hyperviscosity is mainly due to increased erythrocyte aggregation. Compound 4 prevents an increase in blood viscosity at low shear rates both under conditions of blood hyperviscosity *in vitro* (from 2 to 20 revolutions per minute $p < 0.05$ compared to control samples) and under *in vivo* conditions with experimental pulmonary fibrosis induced by bleomycin (from 2 to 12 revolutions per minute $p < 0.05$ compared to control animals).

4. Materials and methods

4.1. Synthesis of compounds

^1H and ^{13}C NMR spectra were recorded on a Bruker DRX400 (400 and 100 MHz, respectively), Bruker AVANCE 500 (500 and 125 MHz, respectively) and Magritek spinsolve 80 carbon ultra (81 and 20 MHz, respectively) instruments using CDCl_3 and $\text{DMSO } d_6$ the internal standard was TMS or residual solvent signals (2.49 and 39.9 ppm for ^1H and ^{13}C nuclei in $\text{DMSO } d_6$; 7.26 and 77.0 ppm for ^1H and ^{13}C nuclei in CDCl_3). Chromato-mass spectrometric studies were carried out on a Trace GC Ultra chromatograph with a DSQ II mass-selective detector in the electron ionization mode (70 eV) on a Thermo TR-5 MS quartz capillary column, 15 m long, 0.25 mm inner diameter, with a film thickness of the stationary phase of 0.25 μm . Splitless input mode was used. Carrier gas discharge 20 ml/min. The velocity of the carrier gas (helium) is 1 ml/min. Evaporator temperature 200 °C, transition chamber temperature 200 °C, ion source temperature 200 °C. The

temperature of the column thermostat was changed according to the program: from 15 (5 min delay) to 220 °C at a rate of 20 °C per minute, to 290° at a rate of 15° per minute. The total analysis time was 30 min. The volume of the injected sample is 1 μl . Chromatograms were recorded in TIC mode. The range of mass scanning is 30–450 amu.

Melting points were determined using a Stuart SMP10 hot bench. Monitoring of the reaction course and the purity of the products was carried out by TLC on Sorbfil plates and visualized using iodine vapor or UV light.

1-(2,4,6-trimethylpyridin-3-yl)ethan-1-one 3 was synthesized according to published procedures (Dornow and Machens, 1947). A mixture of acetylacetone (50 g, 0.5 mol) and ammonium acetate (38.5 g, 0.5 mol) was heated at 80 °C on a water bath for 40 h. the reaction mixture was neutralized with Na_2CO_3 and extracted with benzene (3×20 ml). The combined organic layers were dried over anhydrous Na_2SO_4 and then evaporated in vacuum. The resulting liquid was distilled at reduced pressure (bp. 159–160 °C / 30 mmHg). The output was a slightly yellowish liquid (yield: 25 g (31%)). ^1H NMR (400 MHz, CDCl_3) δ ppm 2.62 s (3H, $-\text{COCH}_3$), 2.84 s (3H, 6- CH_3), 2.88 (s, 3H, 2- CH_3), 2.91 (s, 3H, 4- CH_3), 7.26 (s, 1H, H-5). ^{13}C NMR (101 MHz, CDCl_3) δ ppm 18.1, 21.8, 23.5, 31.5, 121.7, 134.5, 142.0, 151.0, 157.1, 205.7. MS (EI) m/z (I_{rel} , %): $[\text{M}]^+$ 162.99 (43), 147.98 (100), 119.98 (56), 76.96 (16). Anal. calcd for $\text{C}_{10}\text{H}_{13}\text{NO}$: C, 73.70; H, 8.21; N, 8.43; found: C, 73.59; H, 8.03; N, 8.58.

1-(2,4,6-trimethylpyridin-3-yl)ethan-1-ol 4. To a solution of 3-acetyl-2,4,6-trimethylpyridine 3 (2.0 g, 12.0 mmol) in 8 ml of EtOH-water (5:3) was added with stirring in portions NaBH_4 (0.9 g, 24.0 mmol). Stirring was maintained for 2 h after NaBH_4 was all added, then water (50 ml) was added, and the mixture extracted with EtOAc (3×20 ml). The combined organic layers were washed with saturated NaCl solution and dried over anhydrous Na_2SO_4 . The solvent was evaporated under reduced pressure, and the residue was purified by recrystallization from hexane. Yield: 1.8 g (90%), white crystals, mp 94–95 °C. Solubility in water: 10 mg in 0.5 ml of H_2O (pH = 7, at 20 °C). ^1H NMR (500 MHz, CDCl_3) δ ppm 1.48 (d, $J = 6.8$ Hz, 3H, $-\text{CHCH}_3$), 2.38 (2 s, 6H, 4- CH_3 , 6- CH_3), 2.48 (s, 3H, 2- CH_3), 5.28 (q, $J = 6.7$ Hz, 1H, $-\text{CH}$), 6.73 (s, 1H, H-5). ^{13}C NMR (126 MHz, CDCl_3) δ ppm 20.1, 21.8, 23.2, 23.7, 66.3, 124.3, 133.6, 145.7, 154.9, 155.5. MS (EI) m/z (I_{rel} , %): $[\text{M}]^+$ 165.00 (20), 150.04 (100), 122.11 (44). Anal. calcd for $\text{C}_{10}\text{H}_{15}\text{NO}$: C, 72.53; H, 9.37; N, 8.65; found: C, 72.69; H, 9.15; N, 8.48.

(E,Z)-1-(2,4,6-trimethylpyridin-3-yl)ethan-1-one oxime 5. A solution of 3-acetyl-2,4,6-trimethylpyridine 3 (1.0 g, 6.0 mmol), $\text{NH}_2\text{OH}\cdot\text{HCl}$ (1.2 g, 18.0 mmol) and NaOH (0.7 g, 18.0 mmol) in 50% aqueous solution of EtOH (10 ml) was refluxed for 10 h. At the end of the reaction (GC–MS control), the mixture was poured into water and extracted with EtOAc (3×10 ml). The combined organic layers were washed with saturated NaCl solution and dried over anhydrous Na_2SO_4 . The solvent was evaporated under reduced pressure, and the residue was purified by recrystallization from a mixture of hexane: methylene chloride (2:1). Yield: 0.8 g (76%), white crystals, mp 163–165 °C. ^1H NMR (500 MHz, $\text{DMSO } d_6$) δ ppm 1.99 s (1.2H, 6- CH_3 (Z)), 2.00 s (1.8H, 6- CH_3 (E)), 2.06 s (1.2H, 2- CH_3 (Z)), 2.10 s (1.8H, 2- CH_3 (E)), 2.23 s (1.2H, 4- CH_3 (Z)), 2.27 s (1.8H, 4- CH_3 (E)), 2.35 s (1.2H, N = C- CH_3 (Z)), 2.36 s (1.8H, N = C- CH_3 (E)), 6.91 s (0.4H, H-4 (Z)), 6.94 s

(0.6H, H-4 (E)), 10.55 s (0.4H, =N-OH (Z)), 11.07 s (0.6H, =N-OH (E)). ^{13}C NMR (126 MHz, DMSO d_6) δ ppm 15.4 (N = C-CH₃ (E-)), 18.4 (4-CH₃ (Z)), 18.6 (4-CH₃ (E)), 20.0 (N = C-CH₃ (Z-)), 21.8 (2-CH₃ (Z)), 22.2 (2-CH₃ (E-)), 23.5 (6-CH₃ (Z-)), 23.6 (6-CH₃ (E-)), 121.5 (C-5 (Z-)), 121.9 (C-5 (E-)), 128.9 (C-3 (Z-)), 130.4 (C-5 (E-)), 143.4 (C-4 (Z-)), 145.1 (C-4 (E-)), 152.0 (N = C (Z-)), 152.3 (C-6 (Z-)), 153.2 (N = C-CH₃ (E-)), 154.4 (C-6 (E-)), 156.0 (C-2 (Z-)), 156.1 (C-2 (E-)). MS (EI) m/z (I_{rel} , %): $[\text{M}]^+$ 163.07 (100), 161.11 (59), 146.09 (32), 120.07 (31), 80.27 (27), 77.03 (39). Anal. calcd for C₁₀H₁₄N₂O: C, 67.57; H, 7.73; N, 15.60; found: C, 67.39; H, 7.92; N, 15.72.

3-acetyl-2,4,6-trimethylpyridine 1-oxide **6**. To a solution of 1.6 g (10.0 mmol) of 3-acetyl-2,4,6-trimethylpyridine **3** in AcOH (5 ml) was added 5 ml (50.0 mmol) of 30% aqueous solution of H₂O₂. The reaction mixture was refluxed for 5 h. At the end of the reaction (GC-MS control), the mixture was poured into water, neutralized with NaHCO₃ (to pH 6–7) and extracted with EtOAc (3 × 20 ml). The combined organic layers were washed with saturated NaCl solution and dried over anhydrous Na₂SO₄. Concentrating in vacuum gave product as a yellow oily substance. Yield: 1.2 g (70%). ^1H NMR (500 MHz, CDCl₃) δ ppm 2.20 (s, 3H, -COCH₃), 2.43 (s, 3H, 4-CH₃), 2.47 (s, 3H, 6-CH₃), 2.50 (s, 3H, 2-CH₃), 7.03 (s, 1H, H-5). ^{13}C NMR (20 MHz, CDCl₃) δ ppm 15.5, 18.2, 20.9, 31.9, 125.8, 133.2, 137.8, 144.6, 149.2, 202.1. MS (EI) m/z (I_{rel} , %): $[\text{M}]^+$ 178.96 (29), 161.98 (100), 134.03 (18). Anal. calcd for C₁₀H₁₃NO₂: C, 67.19; H, 7.15; N, 7.71; found: C, 67.02; H, 7.31; N, 7.82.

3-acetyl-2,4,6-trimethylpyridin-1-ium chloride **7** was obtained by treating at room temperature 3-acetyl-2,4,6-trimethylpyridine **3** (0.50 g, 3.05 mmol) with conc. HCl solution (5 ml). The reaction mixture was stirring at room temperature for 2 h. After evaporation of water under vacuum, hygroscopic colorless crystals were obtained. Yield: 0.6 g (90%). ^1H NMR (80 MHz, D₂O) δ ppm. 2.47 (s, 3H, -COCH₃), 2.61 (s, 3H, 4-CH₃), 2.67 (s, 3H, 6-CH₃), 2.69 (s, 3H, 2-CH₃), 7.59 (s, 1H, H-5). ^{13}C NMR (20 MHz, D₂O) δ ppm 17.1, 18.6, 19.5, 31.5, 127.0, 137.1, 147.9, 153.0, 155.2, 206.2. Anal. calcd for C₁₀H₁₄NOCl: C, 73.14; H, 8.59; N, 8.53; found: C, 73.01; H, 8.76; N, 8.40.

4.2. Study of hemorheological effects on the model of blood hyperviscosity *in vitro*

Hyperviscosity syndrome (HBIS) was reproduced *in vitro* by blood incubation at 43.0 °C for 60 min. Blood viscosity was measured on a Brookfield DV2T rotational viscometer at various spindle speeds (from 2 to 60 rpm). Studies of the hemorheological activity of 5 samples were carried out on 15 Wistar female rats, 12 weeks old, weighing 220–240 g. After blood sampling, the initial blood viscosity was determined in laboratory animals, and then blood samples were incubated with the test substances at a temperature of 43.0 °C for 60 min and then measured the parameters under study. The blood was incubated with the test objects dissolved in DMSO; the final concentration of the compounds was 10–5 g/mL of blood. Blood samples to which DMSO solvent was added in an equivalent amount served as controls. As a reference drug, a substance with known hemorheological properties, pentoxifylline, was used at a concentration of 10–5 g/mL of blood (Plotnikov

et al., 2017). Blood incubation for 1 h under these conditions was accompanied by the formation of blood hyperviscosity (Plotnikov et al., 1996). The initial blood viscosity from each animal was measured once; the blood viscosity after incubation was measured in two samples from each animal, both in control and experimental samples.

4.3. Fibrosis. Study design

The study of the antifibrotic effect of compound **4** was carried out on 12 Wistar male rats, 12 weeks old, weighing 280–320 g. Rats were randomly assigned to one of 3 groups, 4 animals in each group. Experimental fibrosis in rats was induced by intratracheal administration of bleomycin (Bleomycin sulfate, British Pharmacopoeia (BP) Reference Standard; BP971) at a dose of 5 mg/kg of rat body weight, once (Moore et al., 2013).

Group I (sham-operated animals) received 250 μl of sterile saline intratracheally once (manipulation control) by analogy with bleomycin. Animals of this group received drinking water intragastrically daily in a volume of 1.0 ml/rat, (manipulation control), starting 1 week after *i.t.* administration of sterile saline for 2 weeks (14 days).

Group II (control) received bleomycin at a dose of 5 mg/kg of rat body weight in 250 μl of sterile saline solution intratracheally once. Animals of this group received drinking water intragastrically daily in a volume of 1.0 ml/rat, (placebo), starting 1 week after *i.t.* administration of sterile saline for 2 weeks (14 days).

Group III (**4**) received bleomycin at a dose of 5 mg/kg of rat body weight in 250 μl of sterile saline intratracheally once. Animals of this group received compound **4** intragastrically daily at a dose of 50 mg/kg rat body weight, starting 1 week after *i.t.* administration of bleomycin for 2 weeks (14 days).

Euthanasia of laboratory animals was carried out 21 days after *i.t.* administration of bleomycin. Blood was taken from euthanized animals for hemorheological studies and lung tissue for histopathological studies. Blood viscosity was measured on a Brookfield DV2T rotational viscometer at various spindle speeds (from 2 to 60 rpm).

4.4. Histopathological studies

After the animals were removed from the experiment, lung tissue cutting (determination of the optimal localization, sample size, cut direction, and number of cuts) was carried out in accordance with (Kittel et al., 2004).

Histological sections (3 μm), including the main bronchi of each lobe, were stained with (1) hematoxylin and eosin for histomorphometric characterization of the general morphological pattern of the lungs, inflammatory pattern and interstitial edema, (2) Masson's trichrome to demonstrate fibrosis, identification of collagen fibers and newly synthesized collagen (3) by Gomory silvering to detect reticulin fibers.

Hematoxylin and eosin staining was used to determine the overall morphological pattern of the lungs, the inflammatory pattern, and interstitial edema. After fixation in 10% formalin, the material was treated with chemical reagents (isopropyl alcohol, xylene, paraffin medium) in a tissue processor according to an established protocol. After orientation of the material in histological cassettes, the material was embedded in

paraffin to form a block for histological cutting of the material.

For histological assessment of pulmonary fibrosis, Masson's trichrome stain was used to detect an increased amount of collagen (Titford, 2009).

For the histological evaluation of reticulin fibers, Gomory silvering was used in accordance with the protocol (Reticulum Stain Kit, 2018). When stained with silver, reticulin fibers appear as thin, dark fibrils, and abnormalities in the reticulin structure that occur in pulmonary fibrosis can be detected (Kittel et al., 2004).

4.5. *Histomorphometric assessment of the degree of fibrosis of the lung tissue*

We assessed the degree of fibrotic lesion of the lungs as the total area of single or overlapping lesions in % of the area of the histological section of the lung. The degree of damage was determined by the maximum picture of damage obtained by histological examination of lung tissue. All results were grouped into 3 grades depending on the total volume of the lesion. The entire surface of each section of the lung was examined at 10x and 20x eyepiece magnification.

Grade 0 (none) was defined as the absence of damage (pulmonary fibrosis) in < 1%. Grade I (mild) was defined as damage (pulmonary fibrosis) of < 10%. Grade II (moderate) was defined as a focal lesion (pulmonary fibrosis) occupying < 30% of lung tissue on histological examination. Grade III (severe) was defined as diffuse damage (pulmonary fibrosis) occupying more than 30% of the lung tissue on histological examination.

4.6. *Histomorphometric assessment of the stage of lung tissue fibrosis*

Fibrosis stage - a pattern of fibrous tissue, which is a different quantitative combination of type I and III collagen, which has a relative staging change in the temporal-spatial relationship, that is, the pattern of fibrous tissue in our study is equivalent to the stage of lung tissue fibrosis.

The stage of damage was assessed in relation to the total degree of the relative ratio of type I collagen and reticulin (type III collagen, immature collagen) to the area of lesions: FL0, the absence of foci of pulmonary fibrosis; FL1 - reticulin more than 80%, type I collagen less than 20%; FL2 - reticulin more than 50%, type I collagen more than 50%; FL3 - reticulin less than 50%, type I collagen more than 50%; FL4 - reticulin less than 20%, type I collagen more than 80%.

4.7. *Histomorphometric evaluation of acute interstitial injury (edema) and active inflammatory pattern*

Morphometric analysis was carried out by two independent researchers without information about the animal's belonging to the group and intervention. Edema was assessed in the perivascular and peribronchial space per 100 vessels.

Quantitative determination of plasma cells and granulocytes (cells of active inflammation) was carried out over the entire area of the cut. The calculation was carried out for 1000 of all cells: less than 1% - no active inflammation; less than 10% of cells - microfocal infiltration, mild inflammation; less than 30% of cells - macrofocal, moderate degree of inflam-

mation; more than 30% of cells - diffuse, pronounced inflammation.

Giant multinucleated cells and active macrophages with intracytoplasmic inclusions (foam cells) were counted per 10 fields of view x200.

4.8. *Cell viability assays*

The cytoprotective properties of the compound **4** were evaluated in the MTT (3-(4,5-dimethylthiazol-2-yl)-2,5-diphenyltetrazolium bromide) test on the neonatal human dermal fibroblasts cell line (Gibco). Compound **4** was studied at concentrations from 0.03125 to 1 mg/ml of cells in nutrient medium. Compound **4** was dissolved in 10% DMSO. 10 µl of the dissolved substance was added to 100 µl of the nutrient medium with neonatal human dermal fibroblasts. Cells in nutrient medium with the addition of 10% DMSO served as controls. After cells were incubated for 24 h with compound **4**, viability was determined in the MTT test using the MTT Cell Proliferation Assay Kit (BioVision) according to the manufacturer's instructions.

4.9. *Ethical considerations*

All research work with laboratory animals was performed in accordance with generally accepted ethical standards for the treatment of animals, based on standard operating procedures that comply with the rules adopted by the European Convention for the Protection of Vertebrate Animals used for Research and other Scientific Purposes (Strasbourg, France, 1986). The study protocol of the project "Search among bio- and synthetic antioxidants for new biologically active substances capable of inhibiting the development of pulmonary fibrosis" was approved on September 8, 2020 (Protocol No. 4) by the Local Ethics Commission of the Republican State Enterprise "National Center for Biotechnology" (IRB00013497 National Center of Biotechnology IRB #1).

4.10. *Data evaluation*

Statistical processing of histomorphometric data was carried out using a spreadsheet Microsoft Excel (from the Microsoft Office 2010 package) and the software package for statistical analysis IBM SPSS Statistics 20.0. The Mann-Whitney test and χ -square were used for pairwise comparison between the two groups. The Kruskal-Wallis test was used to compare several groups. Differences were considered significant if $p < 0.05$.

Statistical processing of the hemorheological data was carried out using the Microsoft Excel program. The results obtained are presented as mean \pm standard error of the mean.

5. Conclusions

Thus, based on laboratory-available 3-acetyl-2,4,6-trimethylpyridine **3**, we carried out chemical modifications at the acetyl group to obtain the appropriate 1-(2,4,6-trimethylpyridin-3-yl)ethan-1-ol **4**, (E,Z)-1-(2,4,6-trimethylpyridin-3-yl)ethan-1-one oxime **5**, N-oxide **6** and hydrochloride **7**. It's can be a possible direction of synthesis for obtaining new structural derivatives of collidine and establishing the "structure-activity" relationship.

The biological screening of the synthesized compounds for hemorheological activity under conditions of blood hyperviscosity *in vitro* showed that pronounced hemorheological activity was established for all three compounds (3, 4, and 5).

After primary screening studies for hemorheological activity, for several objective reasons, we chose compound 4 as a promising object for *in vivo* studies.

Next, we studied the antifibrotic activity of compound 4 in an experimental model of pulmonary fibrosis in rats induced by intratracheal administration of bleomycin. The introduction of bleomycin led to a violation of the histoarchitectonics of the respiratory sections with excessive deposition of extracellular connective tissue matrix (type I and III collagen).

Compound 4 used in the experiment has a unidirectional anti-inflammatory and antifibrotic effect, improving the locoregional histoarchitectonics of lung tissue. The antifibrotic potential may be due, on the one hand, to the normalization of the immunological locoregional microenvironment in the lung tissue and, on the other hand, inhibition of the excessive activity of collagen biosynthesis, inhibition of the maturation of collagen connective tissue fibers and activation of the phagocytic function with resorption of cellular tissue debris.

With experimental pulmonary fibrosis induced by bleomycin, a syndrome of blood hyperviscosity is formed. Compound 4 prevents an increase in blood viscosity both in the *in vitro* model of blood hyperviscosity and *in vivo* in experimental pulmonary fibrosis induced by bleomycin. Compound 4 at physiological concentrations does not have cytotoxic properties in relation to cell culture of neonatal human dermal fibroblasts.

Thus, we have shown that pyridine derivatives, quite simple in synthesis and not described in the literature, obtained in 2 stages from available reagents, can be of great interest for solving important problems of medicinal chemistry and pharmacology. The search for new effective antithrombotic agents is especially relevant in the light of post-COVID problems associated with side effects of residual pulmonary fibrosis.

Funding

This research was funded by the Science Committee of the Ministry of Education and Science of the Republic of Kazakhstan (grant «Search among bio- and synthetic antioxidants for new biologically active substances capable of inhibiting the development of pulmonary fibrosis», Grant no. AP09260159).

Institutional Review Board Statement

IRB00013497 National Center of Biotechnology IRB #1.

Informed Consent Statement

Not applicable.

CRediT authorship contribution statement

Zarina Shulgau: Conceptualization, Methodology, Investigation, Writing – original draft, Funding acquisition. **Alena Stalinskaya:** Methodology, Investigation. **Shynggys Sergazy:** Validation, Investigation, Writing – original draft. **Aigerim Zhulikeeva:** Methodology, Investigation. **Yevgeniy Kamyshanskiy:** Methodology, Investigation. **Alexander Gulyayev:** Conceptualization, Validation. **Yerlan Ramankulov:** Conceptualization, Validation, Writing – original draft,

Writing – review & editing, Supervision. **Ivan Kulakov:** Conceptualization, Validation, Writing – original draft, Visualization.

Declaration of Competing Interest

The authors declare that they have no known competing financial interests or personal relationships that could have appeared to influence the work reported in this paper.

Acknowledgements

Spectrophotometric studies were carried out using the equipment of the Center for Collective Use “Rational Nature Management and Physicochemical Research” of University of Tyumen.

Sample availability

Samples of the compounds are available from the authors.

Appendix A. Supplementary material

Supplementary data to this article can be found online at <https://doi.org/10.1016/j.arabjc.2023.104821>.

References

- a Costa, C.F., de Souza, M.V., da Silva Lourenço, M.C., Coimbra, E. S., da Silva Lourenço Carvalho, G., Wardell, J., Calixto, S.L., da Trindade Granato, J., 2020. Synthesis and SAR study of simple aryl oximes and nitrofuranyl derivatives with potent activity against mycobacterium tuberculosis. *Lett. Drug Des. Discov.* 17, 12–20.
- Abblard, J., Decoret, C., Cronenberger, L., Pacheco, H., 1972. Preparation et détermination de structure de nouvelles pyridines halogénées Mécanisme de l'halogénéation. *Bull. Soc. Chim. Fr.* 6, 2466–2481.
- Abele, E., Abele, R., Lukevics, E., 2003. Pyridine oximes: synthesis, reactions, and biological activity. *Chem. Heterocycl. Compd.* 39, 825–865.
- Akhtar, W.M., Cheong, C.B., Frost, J.R., Christensen, K.E., Stevenson, N.G., Donohoe, T.J., 2017. Hydrogen borrowing catalysis with secondary alcohols: a new route for the generation of β -Branched carbonyl compounds. *JACS* 139, 2577–2580.
- Alousi, A., Farah, A.E., Leaner, G., Opalka Jr., C.J., 1979. Cardiotonic activity of amrinone–Win 40680 [5-amino-3,4'-bipyridine-6(1H)-one]. *Circulation Res.* 45, 666–677.
- Amirrah, I.N., Lokanathan, Y., Zulkiflee, I., Wee, M.F.M.R., Motta, A., Fauzi, M.B., 2022. A comprehensive review on Collagen Type I development of biomaterials for tissue engineering: from biosynthesis to bioscaffold. *Biomedicines* 10, 2307.
- Asif, M., 2017. A mini review: biological significances of nitrogen hetero atom containing heterocyclic compounds. *Int. J. Bioorganic Chem.* 2, 146–152.
- Available online: (a) <https://go.drugbank.com/drugs/DB00891>; (b) <https://go.drugbank.com/drugs/DB13882>; (c) <https://go.drugbank.com/drugs/DB01438>; (d) <https://go.drugbank.com/drugs/DB00214>; (e) <https://go.drugbank.com/drugs/DB01114>; (f) <https://go.drugbank.com/drugs/DB01628>; (g) <https://go.drugbank.com/drugs/DB00366> (accessed on 21 November 2022).
- Available online: <https://drugs.ncats.io/substance/2R985002CT> (accessed on 21 November 2022).

- Becatti, M., Marcucci, R., Gori, A.M., Mannini, L., Grifoni, E., Liotta, A.A., Sodi, A., Tartaro, R., Taddei, N., Rizzo, S., Prisco, D., Abbate, R., Fiorillo, C., 2016. Erythrocyte oxidative stress is associated with cell deformability in patients with retinal vein occlusion. *J. Thrombosis Haemostasis* 14, 2287–2297.
- Caprari, P., Massimi, S., Diana, L., Sorrentino, F., Maffei, L., Materazzi, S., Risoluti, R., 2019. Hemorheological alterations and oxidative damage in sickle cell Anemia. *Front. Mol. Biosci.* 6, 142.
- Cecchi, E., Mannini, L., Abbate, R., 2009. Role of hyperviscosity in cardiovascular and microvascular diseases. *Giornale Italiano di Nefrologia: Organo Ufficiale Della Societa Italiana di Nefrologia* 26, 20–29.
- De Martino, G., La Regina, G., Di Pasquali, A., Ragno, R., Bergamini, A., Ciaprin, C., Silvestri, R., 2005. Novel 1-[2-(Diarylmethoxy) ethyl]-2-methyl-5-nitroimidazoles as HIV-1 non-nucleoside reverse transcriptase inhibitors. A structure– activity relationship investigation. *J. Med. Chem.* 48, 4378–4388.
- Dornow, A., Machens, H., 1947. Über einige Analoga des Heterovitamin B1. *Chemische Berichte* 80, 502–505.
- Dygai, A.M., Skurikhin, E.G., Andreeva, T.V., Ermolaeva, L.A., Khmelevskaya, E.S., Pershina, O.V., Krupin, V.A., Reztsova, A. M., Stepanova, I.E., Goldberg, V.E., 2011. Reactions of the blood system and stem cells in bleomycin-induced model of lung fibrosis. *Bull. Exp. Biol. Med.* 152, 173–176.
- Fedorov, B.S., Fadeev, M.A., Sinyashin, A.M., Bogdanov, G.N., Mishchenko, D.V., Varfolomeev, V.N., Pat. Of Russian Federation RU2250210C1 2,4,6-trimethyl-3-oxypyridine nitrosuccinate and method for production thereof.
- Fox, H.H., 1952. The chemical approach to the control of tuberculosis. *Science* 116, 129–134.
- Frost, J.R., Cheong, C.B., Akhtar, W.M., Caputo, D.F., Stevenson, N.G., Donohoe, T.J., 2015. Strategic application and transformation of ortho-disubstituted phenyl and cyclopropyl ketones to expand the scope of hydrogen borrowing catalysis. *JACS* 137, 15664–15667.
- Gilmanov, R.Z., Falyakhov, I.F., Petrov, E.S., Filippov, Y.V., Fedorov, B.S., 2012. 3-hydroxy-2,4,6-trimethylpyridine is a promising anti-ischemic drug. *Bull. Technol. Univ.* 15, 82–85.
- Gross, T.J., Hunninghake, G.W., 2001. Idiopathic pulmonary fibrosis. *N. Engl. J. Med.* 345, 517–525.
- Habib, I., Singha, K., Hossain, M., 2023. Recent progress on pyridine N-Oxide in organic transformations: a review. *ChemistrySelect* 8, e202204099.
- Huang, K., Ortiz-Marciales, M., Hughes, D., 2010. Catalytic Enantioselective Borane Reduction of Benzyl Oximes: Preparation of (S)-1-Pyridin-3-yl-ethylamine bis Hydrochloride. *Organic syntheses; an annual publication of satisfactory methods for the preparation of organic chemicals* 87, 36–52.
- Itsuno, S., 1998. Enantioselective Reduction of Ketones. *Organic Reactions*, 395–576.
- Jian, M., Jiajung, F., Zhengren, G., Chen, H., Bo, Y., Fong, W., Duoning, W., Shufen, S., 1993. A new hypothesis about the relationship between free radical reactions and hemorheological properties in vivo. *Med. Hypotheses* 41, 516–520.
- Jokanovic, M., Prostran, M., 2009. Pyridinium oximes as cholinesterase reactivators. Structure-activity relationship and efficacy in the treatment of poisoning with organophosphorus compounds. *Curr. Medicinal Chem.* 16, 2177–2188.
- Kaddouri, Y., Abridach, F., Yousfi, E.B., El Kodadi, M., Touzani, R., 2020. New thiazole, pyridine and pyrazole derivatives as antioxidant candidates: synthesis, DFT calculations and molecular docking study. *Heliyon* 6, e03185.
- Katritzky, A.R.; Lagowski, J.M., 1967. *Heterocyclic N-oxides*, Methuen: London, UK; (b) Ochiai, E., 1967. *Aromatic amino oxides*, Am. Elsevier: New York, USA; (c) Albini, A., 1991. *Pietra S. Heterocyclic N-oxides*, CRC Press Wolfe Publishing: London, UK; (d) Katritzky, A.R., Lam, J.N., 1992. *Heterocyclic N-oxides and N-imides*. *Heterocycles* 33, 1011–1049.
- Kerru, N., Gummidi, L., Maddila, S., Gangu, K.K., Jonnalagadda, S. B., 1909. A Review on recent advances in nitrogen-containing molecules and their biological applications. *Molecules* 2020, 25.
- Kittel, B., Ruehl-Fehlert, C., Morawietz, G., Klapwijk, J., Elwell, M. R., Lenz, B., O'Sullivan, M.G., Roth, D.R., Wadsworth, P.F., 2004. Revised guides for organ sampling and trimming in rats and mice – Part 2: a joint publication of the RITA and NACAD groups. *Experimental Toxicologic Pathol.* 55, 413–431.
- Kulakov, I.V., Nikitina, O.S., Fisyuk, A.S., Goncharov, D.S., Shulgau, Z.T., Gulyaev, A.E., 2014. Synthesis and intramolecular cyclization of N-acyl- and N-allyl-N'-(2-oxo-1,2-dihydro-pyridin-3-yl)thiourea. *Chem. Heterocycl. Compd.* <https://doi.org/10.1007/s10593-014-1519-y>.
- Kulakov, I.V., Matsukevich, M.V., Shulgau, Z.T., Sergazy, S., Seilkhanov, T.M., Puzari, A., Fisyuk, A.S., 2015. Synthesis and antiradical activity of 4-aryl(Hetaryl)-substituted 3-aminopyridin-2 (1H)-ones. *Chem. Heterocycl. Compd.* 51. <https://doi.org/10.1007/s10593-016-1809-7>.
- Kulakov, I.V., Karbainova, A.A., Shulgau, Z.T., Seilkhanov, T.M., Gatilov, Y.V., Fisyuk, A.S., 2017. Synthesis and Analgesic Activity of bis(3,4-dihydroquinoxalin-2(1H)-one) and bis(3,4-dihydro-2H-1,4-benzoxazin-2-one) Derivatives. *Chem. Heterocycl. Compd.* 53, 1094–1097.
- Kulakov, I.V., Palamarchuk, I.V., Shulgau, Z.T., Seilkhanov, T.M., Gatilov, Y.V., Fisyuk, A.S., 2018. Synthesis, structure and biological activity 3-(arylmethyl)aminopyridine-2(1H)-ones and 1H-pyrido[2,3-b][1,4]oxazin-2(3H)-ones. *J. Mol. Struct.* <https://doi.org/10.1016/j.molstruc.2018.04.036>.
- Latif, A.D., Gonda, T., Vágvölgyi, M., Kúsz, N., Kulmány, Á., Ocsosvzki, I., Zomborszki, Z.P., Zupkó, I., Hunyadi, A., 2019. Synthesis and in vitro antitumor activity of naringenin oxime and oxime ether derivatives. *Int. J. Mol. Sci.* 20, 2184.
- Lauber, M.B., Stahl, S.S., 2013. Efficient aerobic oxidation of secondary alcohols at ambient temperature with an ABNO/NOx catalyst system. *ACS Catal.* 3, 2612–2616.
- Lejon, T., Ingebrigtsen, T., Helland, I., 2005. Palladium-catalysed synthesis of pyrimidines. *Heterocycles* 65, 2593.
- Liu, X., Wu, H., Byrne, M., Krane, S., Jaenisch, R., 1997. Type III collagen is crucial for collagen I fibrillogenesis and for normal cardiovascular development. *Proc. Nat. Acad. Sci.* 94, 1852–1856.
- Mashkovsky, M.D., 2017. *Medicines; New Wave: Moscow, Russia*, p. 1216 (in Russian).
- McDougall, P., 2014. *Phillips_McDougall AgriService: Midlothian, UK*, December.
- Melnikov, N.N.P., 1987. *Chemistry, technology and application. Chemistry, Moscow, Russia*, 712. in Russian.
- Moore, B.B., Lawson, W.E., Oury, T.D., Sisson, T.H., Raghavendran, K., Hogaboam, C.M., 2013. Animal models of fibrotic lung disease. *Am. J. Respir. Cell Mol. Biol.* 49, 167–179.
- Nemeth, N., Peto, K., Magyar, Z., Klarik, Z., Varga, G., Oltean, M., Mantas, A., Zoltan Czigany, Z., Tolba, R.H., 2021. Hemorheological and microcirculatory factors in liver ischemia-reperfusion injury—An update on pathophysiology, molecular mechanisms and protective strategies. *Int. J. Mol. Sci.* 1864, 22.
- Oae, S., Ogino, K., 1977. Rearrangements of t-amine oxides". *Heterocycles* 6, 583–675.
- Oleshchuk, A.L., Karbainova, A.A., Krivoruchko, T.N., Shulgau, Z. T., Seilkhanov, T.M., Kulakov, I.V., 2019. Synthesis and biological activity of 3, 5-diacetyl-2, 6-dimethylpyridine derivatives. *Chem. Heterocycl. Compd.* 55, 47–51.
- Oleshchuk, A.L., Shulgau, Z.T., Seilkhanov, T.M., Vasilchenko, A.S., Talipov, S.A., Kulakov, I.V., 2020. Synthesis and biological activity of 4-(Pyridin-3-yl)-2-hydroxy-4-oxobut-2-enoic acid derivatives. *Synlett* 31, 165–170.
- Palamarchuk, I.V., Shulgau, Z.T., Kharitonova, M.A., Kulakov, I.V., 2021. Synthesis and neurotropic activity of new 3-(arylmethyl)aminopyridine-2(1H)-one. *Chem. Pap.* <https://doi.org/10.1007/s11696-021-01696-7>.

- Paul, G.M., Tambara Filho, R., Repka, J.C.D., 2014. Qualitative analysis of the deposit of collagen in bladder suture of rats treated with tacrolimus combined with mycophenolate-mofetil. *Int. Braz. J. Urol.* 40, 257–265.
- Plotnikov, M.B., Koltunov, A.A., Aliyev, O.I., 1996. Method of selection of medicinal substances affecting the rheological properties of blood in vitro. *Exp. Clin. Pharmacol.* 6, 57–58.
- Plotnikov, M.B., Aliev, O.I., Plotnikova, T.M., 2011. Methodological approaches to studying substances influencing blood rheology. *Eksp. Klin. Farmakol.* 74, 36–39.
- Plotnikov, M.B., Shamanaev, A.Y., Aliev, O.I., Sidekhmenova, A.V., Anishchenko, A.M., Arkhipov, A.M., 2017. Pentoxifylline treatment enhances antihypertensive activity of captopril through hemorheological improvement in spontaneously hypertensive rats during development of arterial hypertension. *J. Am. Soc. Hypertens.* 11, 768–778.
- Rathinasabapathy, A., Bryant, A.J., Suzuki, T., Moore, C., Shay, S., Gladson, S., West, J.D., Carrier, E.J., 2018. rhACE2 Therapy Modifies Bleomycin-Induced Pulmonary Hypertension via Rescue of Vascular Remodeling. *Front. Physiol.* 9, 271.
- Reticulum Stain Kit (Modified Gomori's) For the Histological Visualization of Reticular Fibers. Version 1 Last updated 27 June 2018 ab236473.
- Roitman, E.V., 2003. Clinical hemorheology in Russian Thrombosis Hemostasis Rheol. 3, 13–27.
- Schepetkin, I.A., Plotnikov, M.B., Khlebnikov, A.I., Plotnikova, T. M., Quinn, M.T., 2021. Oximes: novel therapeutics with anticancer and anti-inflammatory potential. *Biomolecules* 2021 (11), 777.
- Shimanskaya, M.V., Leitis, L.Y., 1989. Plant-protection agents based on compounds of the pyridine series (review). *Chem. Heterocycl. Compd.* 25, 477–485.
- Soldatenkov, A.T., Kolyadina, N.M., Shendrik, I.V., 2001. Fundamentals of Organic Chemistry of Medicinal Substances. Chemistry, Moscow, Russia, 192. in Russian.
- Song, Z., Huang, X., Yi, W., Zhang, W., 2016. One-Pot reactions for modular synthesis of polysubstituted and fused pyridines. *Org. Lett.* 18, 5640–5643.
- Stalinskaya, A.L., Martynenko, N.V., Shulgau, Z.T., Shustov, A.V., Keyer, V.V., Kulakov, I.V., 2022. Synthesis and antiviral properties against SARS-CoV-2 of Epoxybenzoxocino [4, 3-b] pyridine derivatives. *Molecules* 27, 3701.
- Stepanenko, V., De Jesús, M., Correa, W., Guzmán, I., Vázquez, C., Ortiz, L., Ortiz-Marciales, M., 2007. Spiroborate esters in the borane-mediated asymmetric synthesis of pyridyl and related heterocyclic alcohols. *Tetrahedron Asymmetry* 18, 2738–2745.
- Titford, M., 2009. Progress in the development of microscopical techniques for diagnostic pathology. *J. Histotech.* 32, 9–19.
- Truppo, M.D., Pollard, D., Devine, P., 2007. Enzyme-catalyzed enantioselective diaryl ketone reductions. *Org. Lett.* 9, 335–338.
- Van Rijn, P.J., 1926. *Recueil des Travaux Chimiques des Pays-Bas et de la Belgique* 45, 267–270.
- Ward, A., Brogden, R.N., Heel, R.C., Speight, T.M., Avery, G.S.A., 1983. A preliminary review of its pharmacological properties and therapeutic use. *Drugs* 26, 468–502.
- Williamson, J.D., Sadofsky, L.R., Crooks, M.G., Greenman, J., Hart, S.P., 2016. Bleomycin increases neutrophil adhesion to human vascular endothelial cells independently of upregulation of ICAM-1 and E-selectin. *Experimental Lung Research* 42, 397–407.